ISSN 0020-1685, Inorganic Materials, 2018, Vol. 54, No. 8, pp. 760–766. © Pleiades Publishing, Ltd., 2018.
Original Russian Text © M.V. Gapanovich, M.D. Agapkin, I.N. Odin, V.V. Rakitin, D.M. Sedlovets, A.M. Kolesnikova, G.F. Novikov, 2018, published in Neorganicheskie Materialy, 2018, Vol. 54, No. 8.

Effect of Precursor Mixture Composition on the Phase Composition and Electrical Transport Properties of $Cu_{1.85}ZnSnS_4$ and $Cu_{1.5}Zn_{1.15}Sn_{0.85}S_4$ Kesterite Solid Solutions Prepared in Molten KI

M. V. Gapanovich[a], M. D. Agapkin[a], I. N. Odin[b, *], V. V. Rakitin[a], D. M. Sedlovets[c], A. M. Kolesnikova[a], and G. F. Novikov[a]

[a] *Institute of Problems of Chemical Physics, Russian Academy of Sciences, pr. Akademika Semenova 1, Chernogolovka, Moscow oblast, 142432 Russia*

[b] *Faculty of Chemistry, Moscow State University, Moscow, 119991 Russia*

[c] *Institute of Microelectronics Technology and High-Purity Materials, Russian Academy of Sciences, Institutskaya ul. 6, Chernogolovka, Moscow oblast, 142432 Russia*

**e-mail: i.n.odin@mail.ru*

Received December 6, 2017; in final form, March 2, 2018

Abstract—We have studied the effect of precursor mixture composition on the phase composition and electrical transport properties of $Cu_{1.85}ZnSnS_4$ and $Cu_{1.5}Zn_{1.15}Sn_{0.85}S_4$ solid solutions with the kesterite structure, prepared by reacting binary sulfides and sulfur in molten KI, and found conditions for the synthesis of $Cu_{1.85}ZnSnS_4$ and $Cu_{1.5}Zn_{1.15}Sn_{0.85}S_4$ solid solutions free from inclusions of impurity phases. The $Cu_{1.5}Zn_{1.15}Sn_{0.85}S_4$ and $Cu_{1.85}ZnSnS_4$ solid solutions have been shown to be *p*-type semiconductors.

Keywords: KI melt, solid solutions, $Cu_{1.5}Zn_{1.15}Sn_{0.85}S_4$, $Cu_{1.85}ZnSnS_4$, unit-cell parameters, electrical transport properties

DOI: 10.1134/S002016851808006X

INTRODUCTION

In recent years, the fabrication of solar cells has been the subject of intense attention in the world [1]. The most promising inorganic materials for such devices include solid solutions based on the Cu_2ZnSnS_4 (CZTS) compound, which has the kesterite structure [2]. However, the efficiency of CZTS-based devices does not exceed 12%, whereas their theoretical efficiency is about 30%. The main cause of this is that single-phase films of CZTS-based solid solutions with predetermined composition are difficult to produce. An interesting alternative is so-called powder-based photovoltaics, which relies on the use of monograin CZTS powders [3]. Such materials are possible candidates for application in building photovoltaics, which integrates buildings and solar cells, and in the fabrication of solar cells. Monograin CZTS powders are typically synthesized in molten salts (KI, CsI, and others) using various precursors. Note that, in the fabrication of solar cells, use is made of copper-deficient, *p*-type solid solutions with the kesterite structure. Kauk et al. [4] described the synthesis of $Cu_{1.8}Zn_{1.05}Sn_{0.95}S_4$ kesterite powders and examined the effect of annealing in sulfur and tin disulfide vapor on their properties. Their results demonstrate that such treatments lead to changes in stoichiometry and improve the efficiency of solar cells [4]. Timmo et al. [5] used a similar procedure to synthesize CZTS samples with Cu/(Zn+Sn) ~ 0.9 and Zn/Sn = 0.96–1.02. Pawar et al. [6] prepared monograin CZTS powders using a starting mixture consisting of binary sulfides, elemental sulfur, and KI.

In this paper, we report the synthesis of $Cu_{1.5}Zn_{1.15}Sn_{0.85}S_4$ and $Cu_{1.85}ZnSnS_4$ kesterite solid solutions, which have not been investigated previously. Our purpose was to assess the influence of the relationship between binary sulfides, sulfur, and KI in the precursor mixture on the phase composition and electrical transport properties of the resultant $Cu_{1.5}Zn_{1.15}Sn_{0.85}S_4$ and $Cu_{1.85}ZnSnS_4$ solid solutions.

EXPERIMENTAL

Starting chemicals. In our preparations, we used copper, tin, and zinc of 4N purity; OSCh 16-5 sulfur; and extrapure-grade $ZnSO_4 \cdot 7H_2O$ and KI.

Synthesis of the binary sulfides. CuS, Cu_2S, SnS, and SnS_2 were synthesized by reacting Cu, Sn, and S

Table 1. CZTS synthesis schemes

No.	Synthesis scheme
	$Cu_{1.5}Zn_{1.15}Sn_{0.85}S_4$
1	$1.5CuS + 1.15ZnS + 0.85SnS + 0.5S \xrightarrow{2KI} Cu_{1.5}Zn_{1.15}Sn_{0.85}S_4$
2	$1.5CuS + 1.15ZnS + 0.85SnS + 0.5S \xrightarrow{5KI} Cu_{1.5}Zn_{1.15}Sn_{0.85}S_4$
3	$1.5CuS + 1.15ZnS + 0.85SnS + 0.5S \xrightarrow{15KI} Cu_{1.5}Zn_{1.15}Sn_{0.85}S_4$
4	$1.5CuS + 1.15ZnS + 0.35SnS + 0.5SnS_2 \xrightarrow{2KI} Cu_{1.5}Zn_{1.15}Sn_{0.85}S_4$
5	$1.5CuS + 1.15ZnS + 0.35SnS + 0.5SnS_2 \xrightarrow{5KI} Cu_{1.5}Zn_{1.15}Sn_{0.85}S_4$
	$Cu_{1.85}ZnSn_0S_4$
6	$0.925Cu_2S + SnS_2 + ZnS + 0.075S \xrightarrow{5KI} Cu_{1.85}ZnSnS_4$
7	$0.85Cu_2S + 0.15CuS + ZnS + SnS_2 \xrightarrow{2KI} Cu_{1.85}ZnSnS_4$
8	$Cu_{1.85}ZnSn + 4S \longrightarrow Cu_{1.85}ZnSnS_4$

in several steps. In the first step, appropriate elemental mixtures were fired at 800°C for 24 h in graphitized silica ampules pumped down to p_{res} = 1 Pa. Next, the products were ground in an agate mortar and the powders were again placed in evacuated silica ampules and annealed for 100 h. The annealing temperature was 800°C for Cu_2S, SnS, and SnS_2 and 450°C for CuS.

Since reaction between zinc and sulfur is too vigorous, ZnS was prepared by bubbling hydrogen sulfide through an aqueous $ZnSO_4$ solution with the addition of CH_3COONH_4 for 5 h. The resultant precipitate was then washed with an aqueous 2% CH_3COOH solution saturated with H_2S. The zinc sulfide was filtered off under vacuum in a glass filter funnel. Next, it was annealed in three steps: in flowing nitrogen at 800°C, in hydrogen sulfide at 600°C, and under dynamic vacuum at 600°C.

Synthesis of CZTS samples. CZTS was synthesized according to the reaction schemes presented in Table 1. The CZTS : KI ratio in the starting mixture was varied from 1 : 2 to 1 : 15 (Table 1). We also varied the ratio between the binary sulfides and sulfur so as to obtain $Cu_{1.5}Zn_{1.15}Sn_{0.85}S_4$ or $Cu_{1.85}ZnSnS_4$. Prior to synthesis, appropriate mixtures of the starting chemicals, corresponding to the reaction schemes in Table 1, were ground and then fired in evacuated graphitized silica ampules for 100 h at 750°C. At high KI concentrations in the mixtures (n_{KI} = 5–15), the powders were prepared as isolated grains in a potassium iodide mass. At n_{KI} = 2, the samples consisted of agglomerates of particles. After the firing, the synthesis products were washed with deionized water to remove KI and dried in vacuum.

Sample *8* was prepared using elemental sulfur and a metallic alloy with the overall composition $Cu_{1.8}ZnSn$, without adding potassium iodide. The ampule as heated to 1120°C over a period of 6 h and then held at this temperature for 10 h. The synthesis products were homogenized at 750°C for 100 h.

Characterization techniques. The phase composition and unit-cell parameters of the samples were determined by X-ray diffraction. Diffraction patterns were collected on an ADP-2-01 diffractometer with Ni-filtered CuK_α radiation.

Since the diffraction peaks of CZTS coincide with those of the ZnS impurity phase [3], the phase composition of the samples was also determined by Raman spectroscopy using a Bruker Senterra micro-Raman system (532 nm). This method allows zinc sulfide to be identified in mixtures with CZTS.

The electrical transport properties of CZTS were studied by a photoelectrochemical (PEC) method. This method is based on reversible reduction of ions in an electrolyte by photogenerated current carriers present in a semiconductor under illumination [6–8]. It has recently been used by different researchers to study photosensitive semiconductor films for photovoltaic applications [6–8].

The electrical transport properties of a monograin CZTS powder are rather difficult to study without destroying its structure. To study them by "classic" voltammetric techniques, it is necessary to make contacts after pressing or sintering the powder, which will inevitably change its structure. The PEC method is free from this drawback, because an aqueous salt solution is used as one of the contacts. The counter electrode and electrolyte concentration were adjusted so that the illumination-induced change in the electrical resistance of the electrochemical cell was determined primarily by the film under investigation. The formation of photogenerated current carriers is the most important process in the absorbing layer of a solar cell (in the CZTS layer in our case). The PEC method

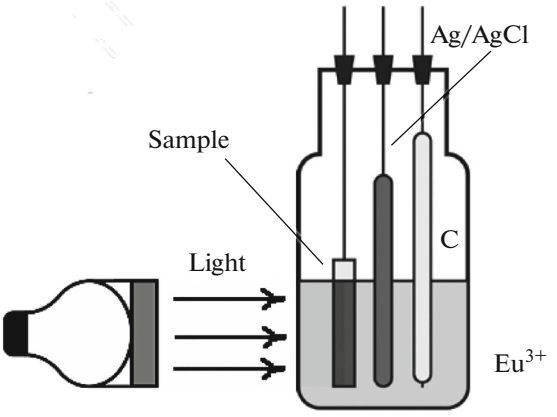

Fig. 1. Schematic of the photoelectrochemical cell: C, graphite counter electrode; silver/silver chloride electrode in the center and working electrode on the left.

allows one to study processes related to the formation of photogenerated current carriers.

The electrolyte solution contains a cyanoacrylate adhesive/CZTS film, which produces photogenerated current carriers under illumination. Cyanoacrylate adhesive is a dielectric, so under illumination with low-energy photons (1.5–2 eV in our case) the formation of photogenerated current carriers in it is quite unlikely. Current carriers are photogenerated predominantly in the CZTS semiconductor, which has a band gap E_g in the range 1.3–1.45 eV (the E_g of CZTS was evaluated from cathodoluminescence data, which will be presented in a subsequent report). As a result, the electrical resistance value obtained refers to the material that produces photogenerated current carriers under illumination, that is, to CZTS semiconductor. Thus, taking into account how the electrolyte concentration and the nature of the counter electrode in the electrochemical cell were chosen, we conclude that the electrical resistance values obtained under illumination are associated primarily with the CZTS powder.

Figure 1 shows a schematic of the photoelectrochemical cell used. An aqueous solution of a Eu^{3+} salt is typically used as an electrolyte [6–8]. A potential sweep is applied to the electrodes, and pulsed light is used.

Prior to PEC characterization, the powders were mixed with cyanoacrylate adhesive in the weight ratio 2 : 1. The resultant mixtures were evenly applied to a substrate (glass/2 μm Mo) 1.5 cm^2 in area and dried for 24 h.

The measurements in the PEC cell were performed in a three-electrode configuration, with a glass/Mo/(CZTS + adhesive) working electrode (to increase the shunt resistance, the edges of the samples were additionally insulated with cyanoacrylate adhesive), graphite counter electrode, and ESr-10101 silver/silver chloride electrode as a reference (potential of +212 mV vs. a standard hydrogen electrode). A reference electrode was necessary because the absolute potential of an individual electrode could not be measured.

The electrical resistance of the films was evaluated under the assumption that, since they were similar in composition and contained no (or negligible amounts of) impurity phases, the potentials of the films vs. the reference electrode differed little, so no correction for the electrode potential of the material under investigation was needed.

The electrolyte used was an aqueous 0.2 M $Eu(NO_3)_3$ solution. According to preliminary results and analysis of the literature, the optimal concentration of aqueous $Eu(NO_3)_3$ solutions used as electrolytes is 0.1–0.3 M. At lower concentrations, the resistance of the electrolyte increases, leading to poorer accuracy in determining the resistance of the semiconductor film. Higher concentrations are not required.

Current–voltage curves were recorded using an IPC Pro potentiostat/galvanostat (I_{min} = 1 μA , E_{min} = 1 mV) and the corresponding software suite. The potential sweep rate was 10 mV/s. The samples were illuminated with pulsed light (τ = 10 s) with a spectrum approaching the solar spectrum in the Earth's atmosphere.

RESULTS AND DISCUSSION

Phase composition and unit-cell parameters of CZTS. Figure 2 shows X-ray diffraction patterns of the CZTS samples synthesized at different starting-mixture compositions. Table 2 lists the unit-cell parameters of the samples (tetragonal symmetry, kesterite structure).

$Cu_{1.5}Zn_{1.15}Sn_{0.85}S_4$ solid solution. All of the reflections in the X-ray diffraction patterns of samples *1* and *5* correspond to a CZTS phase with the kesterite structure (Fig. 2). No reflections from impurity phases were detected. The unit-cell parameters of sample *1* are essentially identical to those of sample *5* (Table 2).

Analysis of Raman spectra (Fig. 3) indicated that a number of samples contained, in addition to the kesterite phase (peaks at 288, 338, and 368 cm^{-1}), small amounts of the stannite phase of CZTS (peak at 318 cm^{-1}) and the ZnS phase (352 cm^{-1}). The ZnS phase was detected in samples *2* and *3* (Fig. 3).

The $Cu_{1.5}Zn_{1.15}Sn_{0.85}S_4$ solid solution is enriched in Zn compared to Cu_2ZnSnS_4. Because of this, a number of precautions should be taken to avoid the formation of ZnS as a second phase. In runs *2* and *3* (Table 1), where large amounts of potassium iodide were used, the final product contained ZnS as a second phase. The reason for the formation of the ZnS phase is that crystalline zinc sulfide has a higher bond ionicity than do tin and copper sulfides, so ZnS solubility in molten

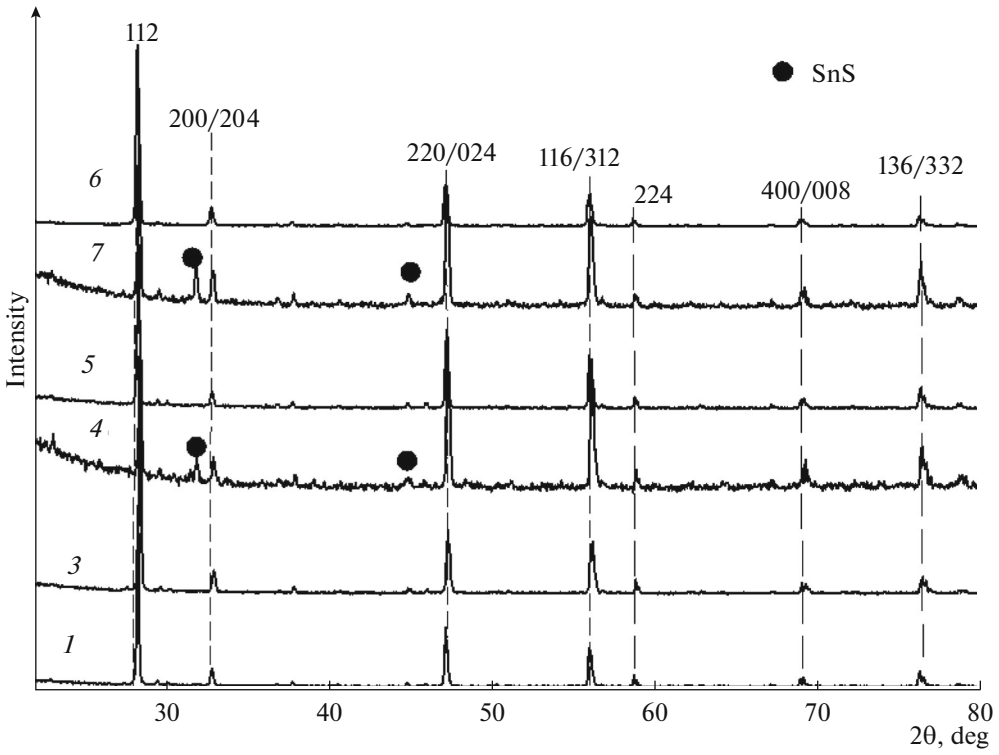

Fig. 2. X-ray diffraction patterns of the samples. (The numbers of the scans correspond to the numbers of the reaction schemes in Table 1.)

KI is higher. During cooling, ZnS crystallizes from the melt to form a second phase. Note that ZnS content increases with increasing KI concentration in the starting mixture. At low KI concentration in the starting mixture (Fig. 3, sample *1*, $n_{KI} = 2$), no ZnS was detected. Thus, the starting mixture for $Cu_{1.5}Zn_{1.15}Sn_{0.85}S_4$ synthesis should contain an amount of sulfur and the minimum possible amount of KI ($n_{KI} = 2$).

If the starting mixture contains no sulfur, the reaction $SnS(s) + 1/mS_m(v) = SnS_2(s)$ does not occur, and some of the SnS subsequently forms a second phase. This is observed for sample *4*. It is of interest to note that SnS as a second phase is formed at low KI concentration in the starting mixture (Fig. 2, sample *4*, $n_{KI} = 2$). At high KI concentration in the starting mixture (sample *5*, $n_{KI} = 5$), no SnS was detected in the final product (Fig. 2).

$Cu_{1.85}ZnSnS_4$ solid solution contains less zinc than does $Cu_{1.5}Zn_{1.15}Sn_{0.85}S_4$, so no ZnS is formed (Table 2, samples *6*, *7*). The precipitation of SnS as a second phase in sample *7* depends on the KI content of the melt. At the lowest KI content ($n_{KI} = 2$), the SnS phase

Table 2. Unit-cell parameters of the synthesized CZTS samples

No.	Formula or designation	Second phase	a (± 0.005), Å	c (± 0.01), Å	V, Å3
1	$Cu_{1.5}Zn_{1.15}Sn_{0.85}S_4$	–	5.434	10.85	320.23
3	Φ*	ZnS	5.440	10.84	320.63
4	$Φ_1$*	SnS	5.433	10.83	319.64
5	$Cu_{1.5}Zn_{1.15}Sn_{0.85}S_4$	–	5.436	10.85	320.53
6	$Cu_{1.85}ZnSnS_4$	–	5.419	10.87	319.33
7	$Φ_2$**	SnS	5.432	10.83	319.61
–	Cu_2ZnSnS_4	–	5.430	10.84	319.52

* The unit-cell parameters were determined for Φ and $Φ_1$ $Cu_{1.5}Zn_{1.15}Sn_{0.85}S_4$-based phases, after some of the ZnS or SnS precipitated as a second phase.

** The a, c, and V values are given for a $Cu_{1.85}ZnSnS_4$-based phase, after some of the SnS precipitated as a second phase.

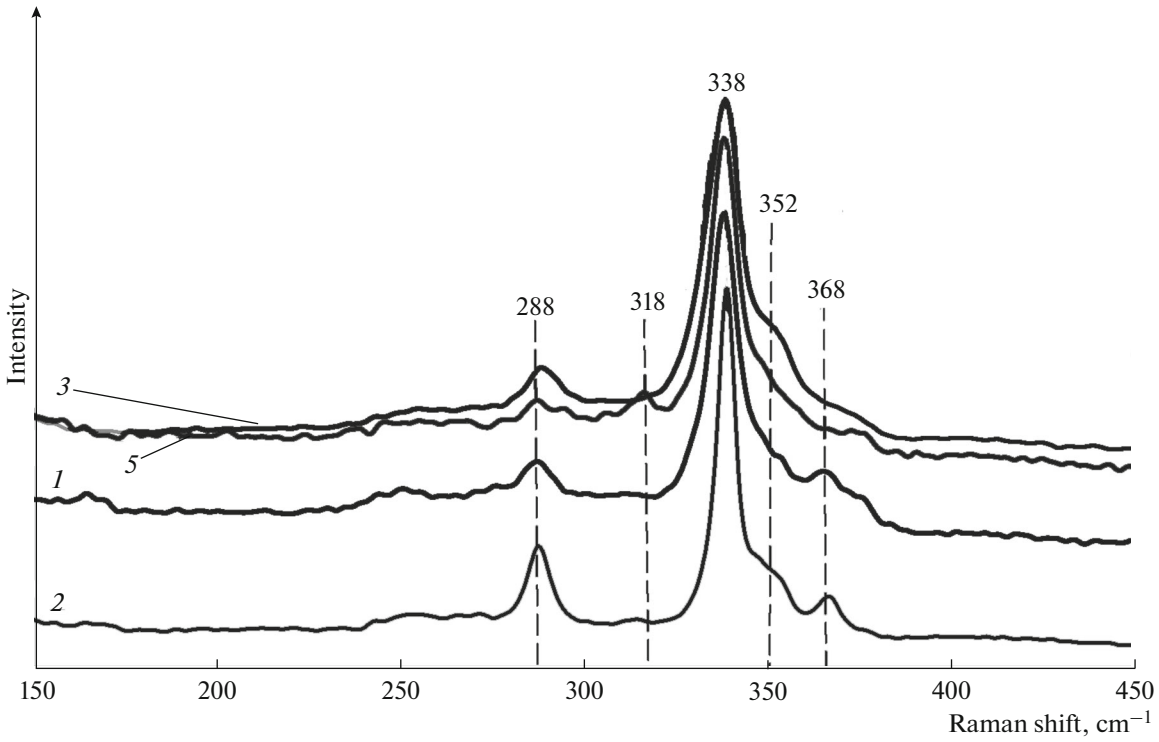

Fig. 3. Raman spectroscopy data. (The numbers of the spectra correspond to the numbers of the reaction schemes in Table 1.)

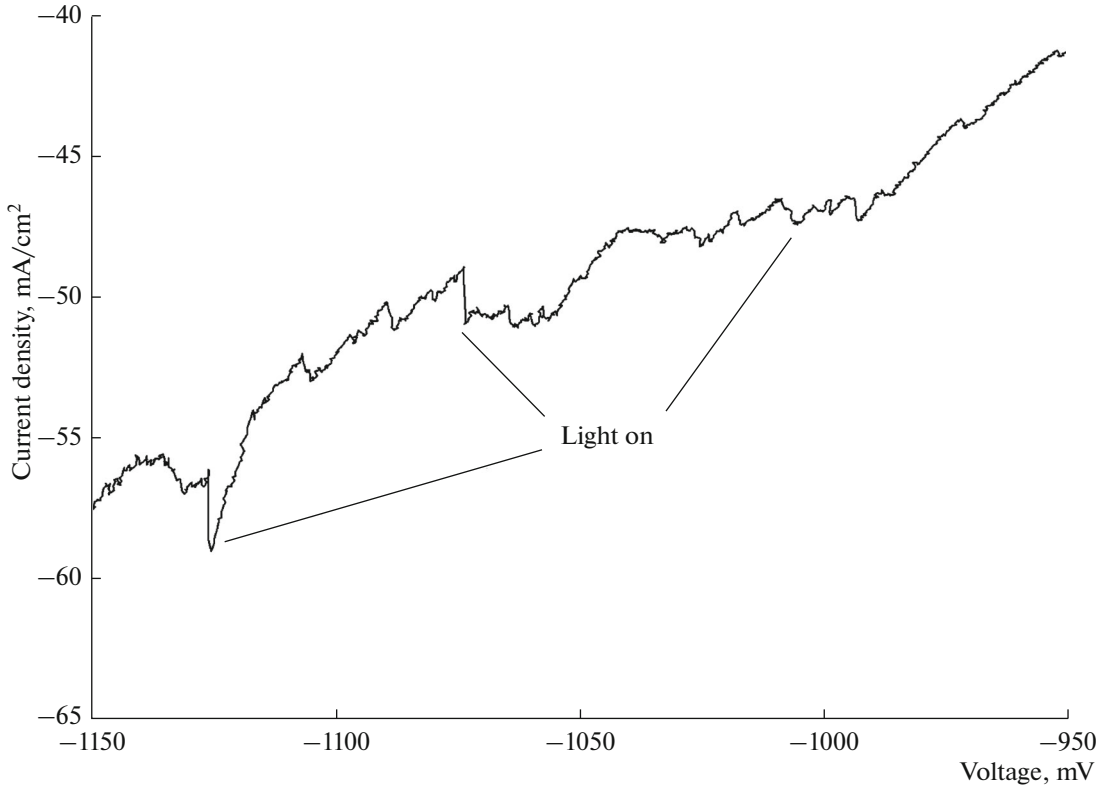

Fig. 4. Portion of the current–voltage curve of the cyanoacrylate adhesive/CZTS (sample *6*) film.

Table 3. Dark resistance R of the cyanoacrylate adhesive/CZTS samples (p-type conductivity)

No.	Formula or designation	R, Ω
1	$Cu_{1.5}Zn_{1.15}Sn_{0.85}S_4$	60 ± 10
2	Φ*	160 ± 20
3	Φ*	140 ± 30
8	$Cu_{1.85}ZnSnS_4$	160 ± 30

* Two-phase samples consisting of ZnS and a $Cu_{1.5}Zn_{1.15}Sn_{0.85}S_4$-based phase.

was present (Fig. 2, sample *7*). At high potassium iodide content (sample *6*), no SnS was detected (Fig. 2). In $Cu_{1.85}ZnSnS_4$ synthesis (sample *7*), the starting mixture contained no tin monosulfide, and the SnS phase in sample *7* resulted from the thermal dissociation of tin disulfide: $SnS_2(s) = SnS(s) + 1/mS_m(v)$. Since neither ZnS nor SnS was detected in sample *6*, the synthesis conditions of this sample (Table 1) should be thought of as optimal.

Photoelectrochemical data. The purpose of this part of our research was to assess the effect of synthesis conditions on the electrical transport properties of the samples.

The photocurrent induced by illumination and the photocurrent density were determined by the PEC method. In this study, the data were normalized to the film area (the vertical axis in Figs. 4 and 5 represents the current density). The films were identical in thickness, so the use of their resistances for comparing them to each other was quite adequate.

The electrical resistance of the CZTS semiconductor was evaluated from the linear portion of its current–voltage curve (Fig. 5) (see below). The data in Fig. 5 were used to determine the conductivity type of the semiconductor in the dark.

Analysis of the present photoelectrochemical data indicates that illumination increases the current density, suggesting the formation of photogenerated current carriers in the samples. It is known that an increase in photocurrent amplitude as the potential shifts to positive values indicates that the semiconductor is n-type in the dark. Similar changes at negative potentials point to p-type conductivity [6–8]. In our case, the photocurrent amplitude was found to increase upon a shift of the potential to negative values, indicating that all of the CZTS semiconductors studied here were p-type in the dark. As an example, Fig. 4 shows a portion of the current–voltage curve of sample *6* and indicates the instants when light was turned on. Unfortunately, the measured photocurrent

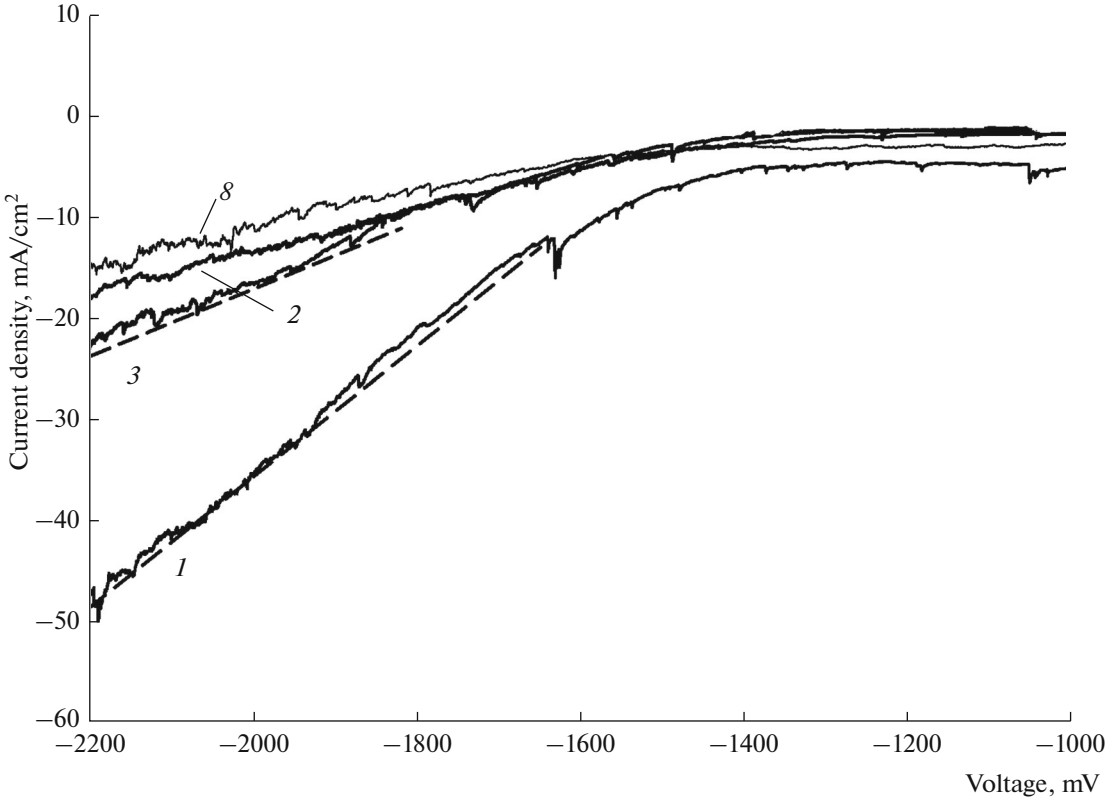

Fig. 5. Evaluation of the electrical resistance of the cyanoacrylate adhesive/CZTS samples from their current–voltage curves in the PEC method. (The numbers of the curves correspond to the numbers of the reaction schemes in Table 1.)

was relatively low in all of the samples. From linear portions (dashed lines) of their current–voltage curves, we evaluated the series electrical resistance R of the samples (Fig. 5, Table 3). The electrical resistance, an important characteristic of an absorbing layer, increases with increasing ZnS concentration in the samples. The reason for this is that zinc sulfide is a high-resistivity material. Also shown in Fig. 5 is the current–voltage curve of $Cu_{1.85}ZnSnS_4$ (sample *8*) prepared by direct synthesis from binary sulfides, without KI in the starting mixture. The R of this sample is 160 Ω (Table 3).

CONCLUSIONS

$Cu_{1.5}Zn_{1.15}Sn_{0.85}S_4$ and $Cu_{1.85}ZnSnS_4$ solid solutions with the kesterite structure have been prepared by reacting copper, zinc, and tin sulfides and sulfur in molten KI. It has been shown that the $Cu_{1.5}Zn_{1.15}Sn_{0.85}S_4$ phase free of ZnS inclusions is formed in the presence of sulfur and at the minimum KI concentration ($n_{KI} = 2$). At higher n_{KI} values in the starting mixture, in the range 5–15, the reaction product contains, in addition to the major, $Cu_{1.5}Zn_{1.15}Sn_{0.85}S_4$-based phase, ZnS, which is due to ZnS solubility in molten KI and ZnS crystallization on cooling.

If the starting mixture contains no sulfur, SnS is formed as a second phase, along with a $Cu_{1.5}Zn_{1.15}Sn_{0.85}S_4$-based phase. At a high potassium iodide concentration in the starting mixture ($n_{KI} = 5$), no SnS is formed during $Cu_{1.5}Zn_{1.15}Sn_{0.85}S_4$ or $Cu_{1.85}ZnSnS_4$ synthesis.

Thus, we have found conditions for the synthesis of $Cu_{1.5}Zn_{1.15}Sn_{0.85}S_4$ and $Cu_{1.85}ZnSnS_4$ solid solutions free of ZnS and SnS inclusions. The present results can be useful for optimizing the synthesis of monograin CZTS powders for the fabrication of membrane solar cells.

$Cu_{1.5}Zn_{1.15}Sn_{0.85}S_4$ and $Cu_{1.85}ZnSnS_4$ have been shown to be p-type semiconductors. Their electrical resistance increases with increasing ZnS concentration, because ZnS is a high-resistivity material.

ACKNOWLEDGMENTS

This work was supported by the Russian Federation Ministry of Education and Science (agreement no. 14.613.21.0065; unique identifier of the project: RFMEF161317X0065).

REFERENCES

1. Luque, A. and Hegedus, S., *Handbook of Photovoltaic Science and Engineering*, New York: Wiley, 2011.
2. Rakitin, V.V. and Novikov, G.F., Third-generation solar cells based on quaternary copper compounds with the kesterite structure, *Usp. Khim.*, 2017, vol. 86, no. 2, pp. 99–112.
3. Copper Zinc Tin Sulfide-Based Thin-Film Solar Cells, Kentaro Ito, Ed., West Sussex: Wiley, 2015.
4. Kauk, M., Muska, K., Altosaar, M., et al., Effects of sulphur and tin disulphide vapour treatments of $Cu_2ZnSnS(Se)_4$ absorber materials for monograin solar cells, *Energy Procedia*, 2011, vol. 10, pp. 197–202.
5. Timmo, K., Kauk-Kuusik, M., Pilvet, M., et al., Influence of order–disorder in Cu_2ZnSnS_4 powders on the performance of monograin layer solar cells, *Thin Solid Films*, 2017, vol. 633, pp. 122–126.
6. Pawar, S.M., Pawar, B.S., Moholkar, A.V., et al., Single step electrosynthesis of Cu_2ZnSnS_4 (CZTS) thin films for solar cell application, *Electrochim. Acta*, 2010, vol. 55, pp. 4057–4061.
7. Damodara Das, V. and Damodare Laxmikant, A study of substrate variation effects on the properties of n-$CdSe_{0.7}Te_{0.3}$ thin film/polysulphide photoelectrochemical solar cells, *Mater. Chem. Phys.*, 1998, vol. 56, pp. 48–55.
8. Pawar, S.M., Moholkar, A.V., Rajpure, K.Y., et al., Electrosynthesis and characterization of CdSe thin films: optimization of preparative parameters by photoelectrochemical technique, *J. Phys. Chem. Solids*, 2006, vol. 67, pp. 2386–2391.

Translated by O. Tsarev